GA–A26481

TOKAMAK ROTATION SOURCES, TRANSPORT AND SINKS

by
J.S. deGRASSIE

JULY 2009

GENERAL ATOMICS

DISCLAIMER

GA–A26481

TOKAMAK ROTATION SOURCES, TRANSPORT AND SINKS

by
J.S. deGRASSIE

This is a preprint of an Invited paper presented at the 36th EPS Conf. on Plasma Physics, in Sofia, Bulgaria, June 29th through July 3, 2009 and to be published in the *Proceedings.*

Work supported by
the U.S. Department of Energy
under DE-FC02-04ER54698

GENERAL ATOMICS PROJECT 30200
JULY 2009

ABSTRACT

Toroidal rotation has become a topic of wide interest experimentally and theoretically because of the recognition that it is important for confinement, stability, and even access to the H-mode confinement regime. The inception of ITER has generated a focus upon developing a prediction for rotation in burning plasmas where auxiliary injected torque will be relatively small. We will describe experimental results and cite theory, organized by sources of toroidal momentum, transport of this momentum, and sinks for momentum, including the effects of some loss of toroidal axisymmetry (AS). We will also describe so-called "intrinsic rotation" where rotation under AS conditions is observed in the absence of any auxiliary momentum source, presumably due to effects such as off-diagonal transport elements, or turbulent stresses, and others. We describe how rotation is measured, and specific areas where the importance of rotation has been established. The predominant source of rotation generation in present devices is the toroidal torque from neutral beam injection. Experiments verify the accuracy of neoclassical (NC) models to describe the torque deposition process in AS conditions. Applied electromagnetic wave power is also found to generate rotation. The radial transport of momentum is found to be much larger than predicted by standard NC theory, having transport rates similar to that of ion thermal energy. Experiments have also verified the existence of a pinch term in the momentum transport, which could generate the interior rotation gradient often observed with intrinsic rotation. The ambient or purposely imposed non-axisymmetric magnetic fields can provide an interior sink for momentum, and that may also drag the rotation to a nonzero offset value. The rotation itself tends to shield out resonant perturbations. Nonresonant perturbations from toroidal field ripple have long been considered, and the area of nonresonant perturbations has taken on new import for the fields generated by perturbation coils for mitigation of edge-localized modes. We consider some of these effects in relation to what might be extrapolated to ITER, but continued experimental and theoretical efforts are required.

I. INTRODUCTION

The pervasive importance of toroidal rotation in the tokamak has been recognized relatively recently, in comparison with issues regarding the plasma particle and energy transport. Tokamak plasmas can exist without toroidal rotation, but not without sufficient particle number or energy content. However, it is now known that sufficient toroidal rotation improves tokamak performance and provides resilience against certain magnetohydrodynamic (MHD) instabilities. This has generated an effort to understand and project toroidal rotation to burning plasmas where the present dominant source of toroidal torque, neutral beam injection (NBI), will be relatively minimal [1], or completely absent.

The role of so-called $E \times B$ rotation shear in enhancing energy confinement is now well established theoretically [2] and experimentally [3]. More recently it has been recognized that rotation, or its shear, has a role in stabilizing MHD instabilities that otherwise limit the achievable β, the plasma energy density normalized to the magnetic energy density. Both the resistive wall mode (RWM) [4] and the neoclassical tearing mode (NTM) [5,6] are ameliorated with toroidal rotation. There is also a role of edge rotation shear in stabilizing the edge localized mode (ELM) phenomenon [7]. Systems are planned for ITER to guard against the degradation due to such potential MHD activity [8]. Knowing the level of rotation that will exist in ITER will impact the ultimate design of such stabilizing systems.

Here we briefly provide an overview of experimental toroidal rotation results in tokamaks, organized roughly according to sources, transport, and sinks of momentum. For this we make reference to early experiments and to some very recent ones. We also make reference to theoretical work on rotation, which has greatly increased in quantity with the realization of the practical import of the topic. We do not have space to give credit to, or cite all the relevant work that has been done, but do try to point to relatively recent publications from which one can start to track backwards through the history of a topic.

We consider a tokamak that is toroidally axisymmetric, or nearly so, to the extent that one can be practically constructed. The application of magnetic perturbation coils has been found advantageous for suppressing ELMs [9], or even actually generating a toroidal rotation [10], yet this breaking of symmetry is still relatively weak in an absolute sense, with $\delta b / B \sim O(10^{-4})$, where δb is the applied vacuum-field perturbation and B the total magnetic field.

Compared with energy, a unique aspect of the topic of momentum is the experimental observation that toroidal rotation exists with no known auxiliary torque injection. This

has been referred to as "spontaneous" rotation [11,12] and "intrinsic" rotation [13,14]. Related is the recent experimental consensus that there exists a pinch term for momentum transport [15–20], just as a particle pinch has been established to provide a peaked density profile with only a boundary source of particles [21-23].

Relative to energy projection scaling, one for toroidal momentum is more difficult due to the vector nature of momentum. Regions of positive and negative toroidal momentum can and do appear within a radial profile, unlike energy and particle density that are positive definite scalars. The pressure profile is further constrained by equilibrium, while the low Mach number toroidal rotations experienced and expected have relatively much less impact upon equilibrium. Strongly driven rotation by neutral beam injection may remove some of this profile ambiguity by being uni-directed. However, with the lesser intrinsic rotation, for example, it may be misleading to use a scalar global momentum to represent the plasma state and we will discuss this in Sec. 5.

II. MEASUREMENT TECHNIQUES

The general tokamak geometry is shown in Fig. 1. The toroidal, V_ϕ, and poloidal, V_θ, fluid velocities are the $\vec{v}$ moment of the distribution function for a particular species projected onto these directions. For mechanical momentum the electron momentum is neglected, owing to the small relative mass.

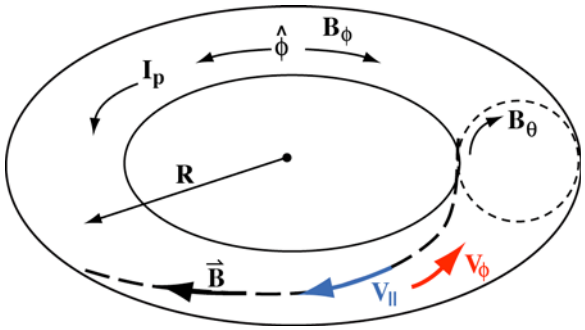

FIG. 1. Toroidal geometry with field directions and toroidal and poloidal directions indicated.

Typically, $M_\phi \equiv V_\phi / \overline{V} \ll 1$. The toroidal rotation at this level in a tokamak, and larger values, is considered to be a constant on a magnetic surface of flux ψ, $\omega_\phi \equiv V_\phi / R$, $\omega_\phi \equiv \omega(\psi)$ [24]. Here, $\overline{V} \equiv \sqrt{T_i / M_i}$, T_i and M_i the ion temperature, and mass. The importance of this is that a poloidally localized measurement of V_ϕ can be extended to the entire surface. There are some experimental data showing that ω_ϕ is constant on a ψ surface [25,26]. Hence, toroidal velocity and toroidal rotation are of habit used interchangeably. Neoclassical theory predicts that V_θ is strongly damped due to the $1/R$ variation of the magnetic field [27]. Only poloidally passing, untrapped ions carry poloidal momentum and such a V_θ is damped by friction with the trapped ions. A relatively small NC V_θ survives in a T_i gradient because the trapped ion friction is then asymmetric in the poloidal direction [27].

Ion velocity, and temperature, are measured spectroscopically. For low-Z_i ions which are fully stripped in typical tokamak conditions, a radiating electron is transiently supplied by NBI, so-called charge-exchange spectroscopy [28] that goes by various acronyms, such as CER. High-Z_i impurity ions are not fully stripped and do not require NBI. X-ray spectrometers are required and the high-Z_i ion must usually be injected for this purpose [29]. Other techniques are used, often to corroborate the spectroscopic measurements. Mach probes can be used in the periphery [30]. The frequency of MHD modes measured with external magnetic probes gives another measure of the toroidal velocity because the mode location can be determined using equilibrium reconstruction,

or temperature fluctuation measurements [31]. This velocity is generally taken to be that of the main, or bulk ion, rather than the low- or high-Z_i minority constituent [31]. One important ongoing research activity is to better understand the relation between the velocities of the various ion constituents in a discharge [32].

The lowest order radial force balance equation is typically used to relate the minority ion velocity measurements to the velocity of the bulk ion [33]. This equation is "radial" in the coordinate normal to the flux surfaces and states $(\vec{E} + \vec{V}_i \times \vec{B} - \vec{\nabla} p_i / Z_i e n_i) \bullet \vec{\nabla}\psi = 0$, for the ith ion species, where p_i is the ion pressure, n_i the density, and $\vec{E}$ the electric field. The minority and bulk ion pressures can be measured as well as the two velocity components for the minority ion (the radial velocity is much smaller). Eliminating the common electric field leaves one equation with two unknowns, the bulk ion V_ϕ and V_θ. A standard procedure is to use NC theory to compute the poloidal velocity and then determine V_ϕ. However, experiments do not always agree with the standard NC result [34], making the usefulness of this approach unclear. Understanding the details of the relatively small tokamak poloidal velocity is another area of ongoing research that impacts a number of intersections between theory and experiment [32].

The validity of the radial force balance equation has been checked in DIII-D by comparing the E field determined from this equation with that due to direct measurement using the motional Stark effect (MSE) diagnostic [35]. In addition, millimeter-wave scattering from turbulent electron density fluctuations gives agreement between the changing E field determined by a changing Doppler shift with that computed from force balance and velocity measurements [36]. Furthermore, Ida has made detailed comparison with E from a heavy ion beam probe in CHS [33].

III. IMPORTANCE OF TOROIDAL ROTATION

In Fig. 2 we show time traces from a DIII-D discharge of the ITER hybrid scenario type [6] that illustrate some points related to the effect of rotation. This is an ELMing H-mode in an upper single null discharge (X-point away from the ion curvature drift). Two of the seven NB sources in DIII-D have been configured to inject toroidally opposite to the others for use in controlled rotation experiments [37]. At $t = 3600$ ms (vertical line) these beams are switched in for others in order to greatly reduce the toroidal velocity, Fig. 2(a), measured for carbon. Our sign convention is that positive V_ϕ is in the direction of the plasma current, I_p. The total NBI power is under feedback control to keep the normalized beta, $\beta_N = \beta aB/I_p$, constant in Fig. 2(b), where the minor radius is a. The total NBI delivered torque is shown in Fig. 2(c) along with the total injected power, P_{inj}. The increase in P_{inj} to maintain constant β_N is necessary because the energy confinement time is reduced at lower rotation, with the H_{89P} energy confinement factor [38] shown in Fig. 2(b). $H_{89P} = 2$ is standard H-mode confinement. At higher velocity ($t < 3600$ ms) the energy confinement exceeded this standard. There is a concomitant reduction in the toroidal momentum confinement as well, as deduced from TRANSP modeling [39,40]. Although the net torque is effectively zero for $t > 3600$ ms, there remains a co-I_p rotation due in part to the intrinsic rotation. The amplitude of a NTM with $m = 3/n = 2$ is seen to increase at lower rotation in Fig. 2(e) [$\delta b \sim \exp(im\theta + in\phi)$]. Lastly, Fig. 2(d) shows the agreement of the measured frequency for δB of this NTM with the $n = 2$ rotational frequency at the $q = 3/2$ surface as measured with CER for the C^{6+} velocity, where $2\pi/q$ is the rotational transform of a flux surface. For the importance of rotation, we take a closer look at the effects seen in Fig. 2 and others.

Experiments have shown that the β_N threshold for the NTM instability depends upon rotation [5]; higher co-rotation is clearly more stable. An electron cyclotron current drive (ECCD) system is planned for ITER to suppress NTMs [41]. A system of feedback-driven coils is planned for ITER to suppress the RWM instability, an issue for the broad toroidal current profiles ultimately anticipated for steady-state, CD operation [4]. Again, rotation provides resilience against the RWM [4]. Another issue for ITER is the transient heat load due to ELMs. In DIII-D an H-mode free of ELMs is being pursued, the QH-mode [42]. Theoretical work indicates that a necessary condition for entering the QH regime may be high toroidal rotation, or rotation shear, near the H-mode pedestal [42]. The power threshold for the L-H transition has also been found to depend upon rotation in controlled DIII-D experiments with torque control [43]; higher co-rotation clearly requires more power for the transition. Understanding this rotation effect may lead to understanding the details of the H-mode transition bifurcation itself.

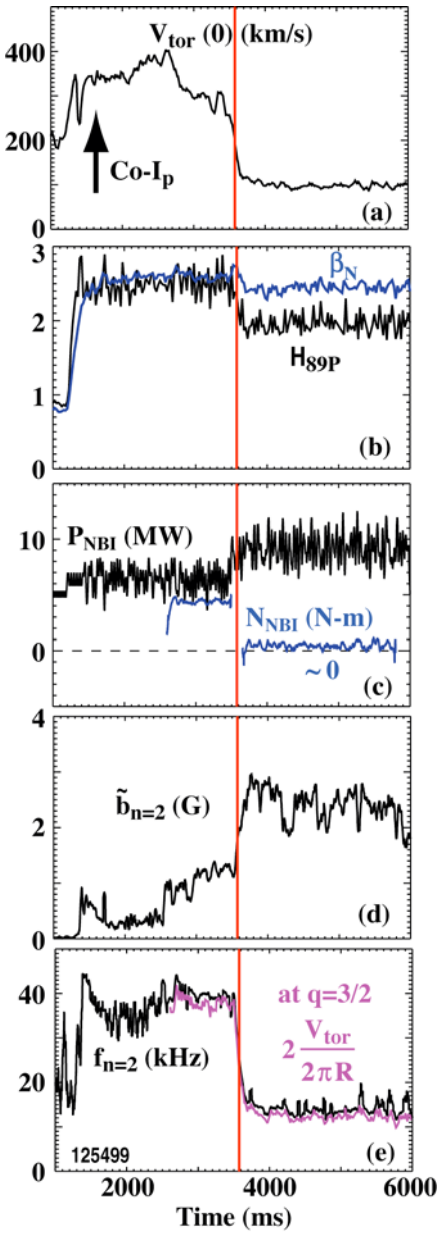

FIG. 2. ELMing hybrid H-mode in DIII-D with a step down in net NBI torque at the time slice marked. (a) Core toroidal velocity (C^{6+}), (b) β_N and H_{89P} factors. Standard H-mode has $H_{89P} = 2$. (c) Total NBI power, P_{NBI}, and total NBI torque, N_{NBI} (d) Externally measured amplitude of $m = 3/n = 2$ tearing mode, (e) Externally measured mode frequency, $f_{n=2}$, and $n = 2$ rotation frequency computed from the C^{6+} measured velocity at the $q = 3/2$ surface.

An early recognition of the importance of rotation came with the understanding that shear in E causes a shear in the $E \times B$ drift motion which elongates and narrows the turbulent eddies that enhance radial energy transport [3]. In the past 20 years a great deal of effort has been devoted to this effect [2]. Apart from a detailed analysis, such an enhancement in confinement would be expected to cause the increased H factor seen in

the high velocity phase of the discharge shown in Fig. 2, due to the $\vec{\mathbf{V}} \times \vec{\mathbf{B}}$ contribution to $\vec{\mathbf{E}}$. The H-mode edge energy transport barrier is believed to exist due to this effect [44], and the plasma velocity is believed to play a role in the bifurcation between the L-mode and the H-mode states [44].

Transport barriers are also found to exist well inside the boundary of a discharge and are called internal transport barriers (ITBs). The toroidal velocity, or shear, can also be a critical feature of an ITB [45]. Recent ITB experiments on JET have shown that high rotation shear is not a necessary condition to trigger an ITB, but the magnitude and temporal resilience of the ITB increase with rotation, or possibly the shear [46]. Figure 3 shows two V_ϕ profiles at the time of ITB formation in these JET experiments, demonstrating the ability to obtain an ITB at relatively low rotation and shear. However, the subsequent ITB in the high velocity condition was twice as steep [46]. The velocity profile is varied here by varying the rotation with the mix of NBI and radio frequency (rf) power. The toroidal field (TF) ripple strength was used to vary the rotation (see Sec. 7) in other JET ITB experiments [46].

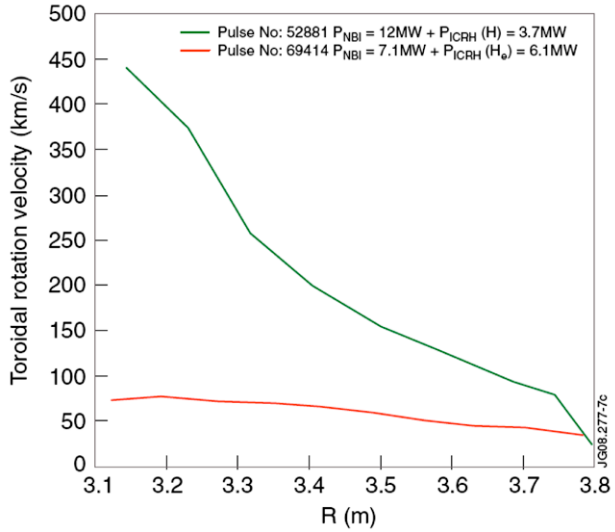

FIG. 3. Toroidal rotation profiles measured at the time of ITB triggering for two discharges in JET [46].

IV. SOURCES

NBI is the dominant source of momentum injection in present-day tokamaks. Mature numerical codes, such as TRANSP, are now routinely used to compute the NBI sources of momentum, energy and particles. One very interesting aspect of NBI momentum delivery is the so-called prompt torque, or "$J_f \times B$" torque, where J_f is the radial current of the fast NBI ions [47-53]. This torque is delivered to the bulk plasma on the timescale of a poloidal transit of a fast ion, typically $\sim$10s of microseconds, while the frictional torque of a fast ion is delivered on the timescale of slowing and scattering from the bulk plasma, typically many 10s of milliseconds, or longer, in large, high temperature tokamaks. The radial fast ion current results from the initial orbital separation of a newly born fast ion from the accompanying electron. In the inertial phase of plasma response, it is the effect of injecting charge into a dielectric [50,51]. With constant canonical toroidal momentum P_ϕ for the bulk plasma, the bulk ion polarization response generates a toroidal drift acceleration in the temporally rising E field, absorbing this prompt fast torque.

In DIII-D this prompt torque has been verified in bulk helium discharges where we measure the velocity of the bulk ion, so that there is no lingering uncertainty in a momentum difference due to measuring a minority ion constituent [50]. Measurements of the change in the toroidal velocity profile across the minor radius agree with the TRANSP-computed impulse due to the prompt torque over a 10 ms time [50]. In this inertial phase the drift nature of the acceleration makes all charged particles respond with equal toroidal velocity change. Measurements show that the prompt velocity change of the C^{6+} ion in the bulk helium discharge equals that for He^{++} [50].

Ultimately the prompt acceleration will be balanced by momentum transport, i.e. the dielectric has finite resistivity, which phenomenologically can be directly related to the momentum confinement time [54]. The frictional torque from a slowing fast ion enters on a longer timescale than the prompt torque and is more susceptible to anomalous effects that modify the fast ion orbits and redistribute the fast ion density profile, such as internal MHD [18], Alfvén eigenmodes [55], and fast ion-driven modes [56]. It has also recently been recognized that electrostatic turbulence can cause anomalous fast ion transport [57]. Of course, NBI heating predominantly also takes place on the frictional timescale (there is some viscous heating due to rotation drive).

An rf wave with nonzero toroidal wave vector also delivers a torque to the bulk plasma, in some scenarios by creating fast ions that deliver the momentum by a process related to the prompt torque effect in NBI. The ratio of injected torque to power is $N/P = n_\phi/\omega$, where n_ϕ is the toroidal wave number and ω the wave frequency. This ratio is typically down nearly 2 or 3 orders of magnitude from that for NBI, but

nevertheless the effect has been measured in JET [58]. Rotation profiles of ω_ϕ were measured with fast Alfvén waves launched in the co- and counter-I_p direction. The co-launch case had more positive ω_ϕ. The difference in ω_ϕ between co- and counter-launch agrees with rf modeling of the wave momentum effect, using a momentum diffusivity that gives equal momentum and energy confinement times (Sec. 6). The counter-launch rotation profile was also in the co-I_p direction, indicating the existence of an intrinsic rotation offset.

Two other novel rf effects have recently been observed to generate, or modify rotation in C-Mod. One results from mode conversion to ion cyclotron waves, called mode conversion flow drive (MCFD) [59], and the other is due to lower hybrid current drive (LHCD) [60]. In both cases explanations are advanced that are based in wave momentum, and particle canonical momentum considerations. These effects will certainly be pursued experimentally and theoretically.

V. INTRINSIC ROTATION

We now turn to intrinsic rotation, observed to exist with no known source of toroidal momentum. It can be closely connected with momentum transport, discussed in the next section, through the momentum pinch effect and off-diagonal elements in the transport matrix.

Intrinsic rotation has been measured experimentally for over 20 years [61], and predicted theoretically nearly as far back [62], but was relatively recently brought to general attention by the work of J.E. Rice and co-workers at C-Mod [63,64]. In a series of experiments Rice organized the intrinsic rotation data by what has become known as Rice scaling [14,63,64], showing that $\Delta V_\phi \propto \Delta W_p / I_p$, where W_p is the total plasma kinetic energy. The Δ is used to indicate the difference from some initial value. The effect spans Ohmic and ICRF H-mode discharges, and the velocity is in the co-I_p direction, a general result for H-mode conditions. Ohmic and L-mode discharges exhibit much greater variety of intrinsic rotation profiles. For example, in TCV Ohmic discharges the toroidal rotation is observed to reverse direction with an increase in the electron density [65]. Yet, limited L-mode discharges in Tore-Supra do exhibit a scaling similar to Rice's [66].

In the early C-Mod intrinsic rotation experiments the velocity measurements were located in the core region in minor radius [67,68]. The peak core velocity was used in the scaling. Here we confront the utility of using the velocity from a single spatial location, or alternatively a scalar global total toroidal momentum, to define the rotational state of the discharge. If the dominant source of toroidal momentum is near the edge of the plasma and transport is via diffusion only, then the momentum profile will be flat internally, and there is no ambiguity. This may describe intrinsic rotation in Ohmic H-modes in DIII-D [69] and so-called enhanced-D_α discharges in C-Mod [68]. With a momentum pinch term added to the transport, the momentum profile can be peaked, or even hollow going toward the magnetic axis. If even relatively small amounts of internal momentum stress are present, especially in the relatively small volume of the core, then virtually any momentum profile can be constructed with the freedom to specify the diffusivity and pinch velocity profiles [70], constrained by a boundary condition. Thus, the physical process under consideration that makes rotation important, for stability or confinement, determines the spatial region of interest.

Focusing intrinsic rotation scaling experiments on H-mode conditions, under dominantly axisymmetric conditions, provides a basis for cross-machine comparisons. Commonly observed is the generation of an increased intrinsic co-V_ϕ, with increased W, as with a transition to H-mode [71]. The Rice scaling is then a natural comparison metric. Additionally, H-mode operation is relevant for burning plasma operation [72]. And it is reasonable to suspect that the strong gradients in the H-mode pedestal play a role in

momentum generation, limiting the source to the edge region. In DIII-D the Rice scaling has been clearly observed, but due to momentum profile effects in rf H-modes, it is only seen in the outer region, inside the pedestal.

In DIII-D experiments on intrinsic rotation in Ohmic and ECH H-modes it is found that the rotation profile is always in the co-I_p direction in the outer region of minor radius, $\rho > 0.5$, but may be co- or counter-I_p inside depending upon the deposition profile of the ECH [14]. The radial coordinate ρ is the normalized square root of the toroidal flux. In analyzing the common co-I_p rotation in the range $0.76 < \rho < 0.81$ (determined by CER measurement channels) the Rice scaling emerged, albeit with a different slope than in C-Mod [14]. These DIII-D data are plotted in Fig. 4(a). In Fig. 4(b) we show a better empirical correlation for these data that includes the ratio of the core region T_e to T_i, where T_e is the electron temperature. These core temperatures may simply be representative of the global temperature gradients. In DIII-D the total V_ϕ is used, not a difference.

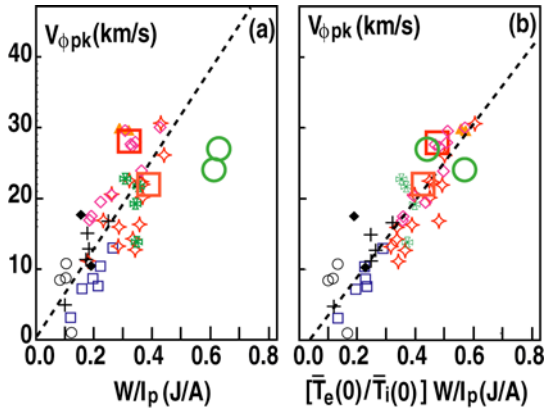

FIG. 4. (a) Rice scaling as found in DIII-D [14] and (b) a modified Rice scaling as found in DIII-D [14]. The large circles are added to the original DIII-D scaling data from $\beta_N \sim 2$ balanced NBI discharges; $\beta_N = 1.85$ (132797.2750) and 1.95 (132797.4600). The large squares from discharges with $\beta_N = 1.0$, (132073.1800) ECH only, and 1.2 (132073.2750) ECH + NBI.

Finding the Rice scaling in DIII-D was a key factor in motivating a similarity experiment between DIII-D and C-Mod. In matching the shape, the value of q_{95} (q at 0.95 in normalized ψ), and core β, the value of M_ϕ agreed between the two devices [14]. In comparing between the two machines in this experiment, the core M_ϕ is used in C-Mod and the M_ϕ value at $\rho \sim 0.8$ in DIII-D [14]. In order to extract a size scaling, many more such dimensionally similar [73] inter-machine experiments are needed.

The Rice scaling has been seen on a number of tokamaks, and an organization of the data in dimensionless parameters has yielded a number of fits [71]. There are limited data that extend up to ITER scenario β_N values, which are at least ~ 1.8, simply because generally the installed rf power (negligible torque) is less than NBI power in most

present-day devices. In DIII-D toroidally "balanced" NBI has been used to augment ECH H-modes, or to replace ECH, in order to raise the β_N value in intrinsic rotation conditions. Due to the opposite prompt orbit shift of co- and counter-I_p NBI ions (J_f) the net local NBI torque density during balanced injection is not zero on all minor radii surfaces, but can be reduced by over an order of magnitude inside the edge region, as compared with directed NBI [14]. In these experiments, small steps in net torque are taken around the nominal balanced condition, at fixed power, in order to measure the response to remnant torque. Values of β_N above 2 have been achieved in this manner.

In Fig. 4(a) we show the plot of the Rice scaling results from discharges in DIII-D with the toroidal velocity taken in the region $\rho \sim 0.8$, V_{pk} [14], the two added large circles are two measurements with balanced NBI to achieve β_N of 1.85 and 1.95. Both of these points fall below the nominal Rice scaling, $V_{pk} \sim W / I_p$, in DIII-D which is taken from Ohmic and ECH H-modes with no NBI torque perturbation and a maximum β_N of approximately 1.3, and $V_{pk} \equiv V_\phi(\rho \approx 0.8)$. With higher β_N and low rotation, tearing modes were present in this discharge [5], and it is necessary to include anomalous fast ion diffusion in TRANSP analyses in order to reduce the computed total neutron rate to that measured. The large squares in Fig. 3(a) are from conditions with lower β_N, no tearing mode activity, and no anomalous fast ion diffusion required for modeling. These added β_N values are 1.0 and 1.19, respectively.

Much more data of this type must be obtained, but a reasonable conclusion could be that the MHD activity, or some type of anomalous transport at the higher β_N could be degrading the achieved co-I_p velocity from the Rice scaling value.

On the other hand, in Fig. 4(b) we plot these same points on the DIII-D modified Rice scaling that includes the ratio of core T_e to core T_i, and find that all points fall well into the original fit [14], independent of β_N. Perhaps MHD activity does not affect intrinsic rotation foremost via transport, but by modifying the temperature profiles that in some way cause the intrinsic rotation. The temperature profiles could affect the turbulence characteristics that underlie the resulting intrinsic rotation as some theories cited in the next section compute.

VI. MOMENTUM TRANSPORT

Neoclassical theory predicts a very small radial diffusivity of toroidal momentum, χ_ϕ, as compared with ion thermal energy, χ_i, because only passing ions carry toroidal mechanical momentum and these orbits do not have the same radial step size enhancement as the trapped orbits, which gives the neoclassical enhancement to energy transport [74.75]. However, experimentally it is well documented that $\chi_\phi \sim \chi_i$ [49,76-78], even in discharges where χ_i approaches the NC value [77]. Turbulent transport is assumed to link these two channels [79,80] and it may be that small levels of turbulence affect momentum transport relatively more than ion energy transport [81]. In stating $\chi_\phi \sim \chi_i$ we mean this crudely, perhaps differing up to a factor of 2 or 3 in quiescent conditions, but nevertheless close compared to the standard NC prediction, where χ_ϕ is a factor of 30 to 100 smaller than χ_i [74].

A general equation for the radial flux of toroidal momentum, Γ_ϕ, used to model experimental conditions has a typical form

$$\Gamma_\phi = -\chi_\phi \frac{\partial \ell}{\partial \rho} + V^p \ell + \left(\mu_{31} \frac{\partial n}{\partial \rho} + \mu_{32} \frac{\partial T}{\partial \rho} + \ldots \right) = S_R + \Gamma_{NBI} + \Gamma_{RF} \quad , \tag{1}$$

where the angular momentum is $\ell = M n_i \langle R^2 \rangle \omega_\phi$, with $\langle\ \rangle$ denoting a flux surface average, and the r.h.s. are source terms, S_R being due to possible turbulent stress source. The existence of a momentum pinch, V^p, is now well established experimentally [15-20]. A significant amount of recent theoretical work deals with the turbulence effects that can produce the V^p, μ_{ij}, and S_R terms, as related to momentum transport and intrinsic rotation [11,82-89]. Off-diagonal terms arise also in neoclassical theories [90-93]. The measured pinch velocity, V^p, in NSTX is compared with the turbulence-based theories of Hahm [85] and Peeters [87] in Fig. 5 [19], showing good agreement. In these experiments both modulated NBI and applied error fields (sinks) were used to perturb the rotation profile [19].

The coupling of the momentum and energy confinement times can explain an effect long seen in tokamaks, namely that the addition of rf heating to a rotating discharge driven by NBI reduces the rotation [94,95]. This is due to the empirically determined power degradation of energy confinement, $\tau_E \sim 1/\sqrt{P}$, where P is the total heating power [96]. The added rf power adds negligible torque but increases P and enhances momentum transport if τ_ϕ scales with τ_E. This model was used by Nishijima, *et al.* to explain experiments on ASDEX-U [97] and we subsequently found it to explain similar results in JET [95]. In a series of experiments in JET, ICRH power was added to target discharges driven with co-I_p and counter-I_p rotation with NBI. The main ion was D^+ and two

heating scenarios were used, minority H and minority ^{3}He. The results relevant to the present topic did not depend upon the heating scenario. Addition of rf power slowed the rotation, and total angular momentum of the plasma [95]. In a simple global steady-state model the total plasma stored energy is $W = P_{aux}\tau$, and the total toroidal momentum is $L = N_{NBI}\tau = sP_{NBI}\tau$, where τ is a common confinement time for energy and momentum, $P_{aux} = P_{rf} + P_{NBI}$ the total auxiliary heating power, N_{NBI} the torque applied and s is the NBI torque to power ratio for the JET NBI utilized. Taking the ratio of L/W, so that the confinement time cancels out, we construct a parameter that should be unity with rf power variation if the simple steady state values with a common τ hold. This parameter is $A \equiv [(1+P_{rf}/P_{NBI})/s](L/W)$ [95]. In Fig. 6 we plot A vs $(1+P_{rf}/P_{NBI})$ for three series of discharges in JET, namely L-mode, high power L- and H-mode, and counter-I_p injection L-mode target discharges obtained during a campaign with the direction of I_p reversed. The flatness of A with variation in P_{rf}/P_{NBI} supports the basic hypothesis that a common power degradation in the confinement of momentum and energy reduces L. The absolute offset from unity could indicate that the ratio of τ_ϕ/τ_E is not unity, i.e., they differ by a multiplier that varies with discharge conditions. The counter-I_p series made it clear that the neglect of intrinsic rotation also contributes to this offset. In our model above, we should be subtracting the intrinsic momentum, L_0, from L (and perhaps including a W_0 with Ohmic heating). With counter-I_p injection L_0 is negative on our scale, in the co-I_p direction. This L_0 value was measured in only one discharge before NBI acceleration resulting in a larger magnitude of $L - L_0$, hence a larger value of the adjusted A, bringing the lower band in Fig. 6 up by roughly 0.25 toward the middle band [95].

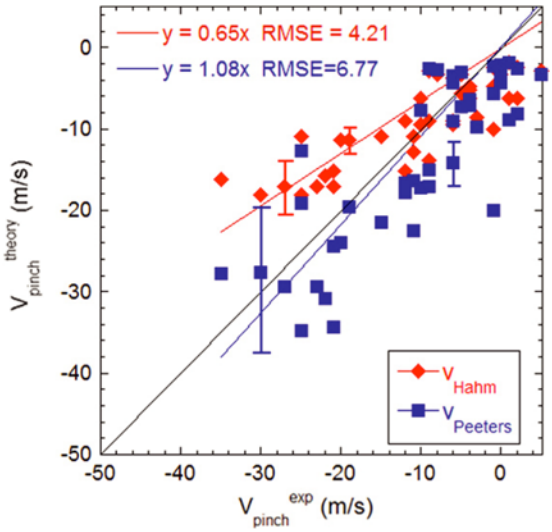

FIG. 5. Theoretical pinch velocities of Hahm [85] (diamond) and Peeters [87] (square) versus those measured in NSTX. [Reprinted with permission from Kaye S M 2009 *Nucl. Fusion* **49**(4) 045010. Copyright 2007, Institute of Physics.]

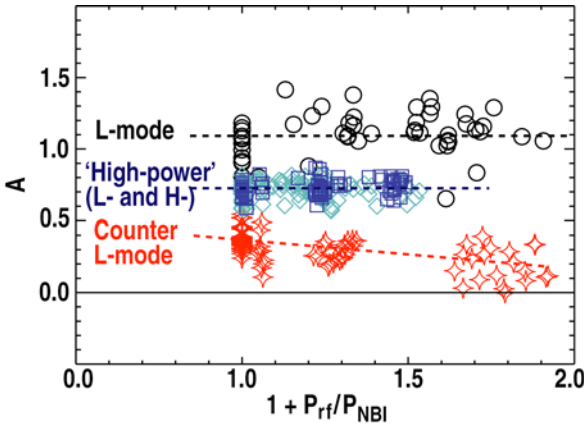

FIG. 6. The "A" parameter defined in the text versus $1+P_{rf}/P_{NBI}$, for JET discharges. Constant A indicates rf slowing is due to the degradation in energy confinement. [Reprinted with permission from deGrassie J S *et al* 2005 *Proc. 16th Top. Conf. on RF Power in Plasmas (Park City)* vol 787, ed S J Wukitch S J and P T Bonoli (Melville, American Institute of Physics) p 110, Copyright 2005, American Institute of Physics.]

The use of a global τ_ϕ and this zero dimensional model are reasonable with the high power uni-directed NBI drive in the target plasma to which rf is applied, as discussed previously. This condition links τ_ϕ and χ_ϕ more tightly than in conditions with significant structure in the momentum profile.

We note that in a recent experiment in JT-60U the addition of EC power reduced the magnitude of the counter-I_p target rotation driven by counter-NBI [98], similar to the lower data band in Fig. 5. As noted there [98] it is important to separate the possible roles of drag, or confinement reduction, and acceleration opposite to the target direction.

The source terms in (1) apart from the known Γ_{NBI} and Γ_{RF} are being sought experimentally in DIII-D. In some H-mode discharges with excess counter-I_p NBI injection, to largely remove the intrinsic rotation, it has been observed that the toroidal velocity is essentially zero over most of the interior of a discharge [18], so that ℓ and $\partial\ell/\partial\rho$ are essentially zero. With $\Gamma_{RF}=0$ in (1), this leaves the off-diagonal terms and S_R to be balanced by Γ_{NBI}, computed with TRANSP. Experiments are underway [18] to test various theories of these remaining terms, especially S_R, using this technique.

VII. SINKS

Breaking axisymmetry leads to enhanced transport [99]. The breaking of axisymmetry may be spontaneous, due to internal MHD activity for example, which can lead to an internal rearrangement of toroidal momentum [77,100], sometimes observed experimentally as a flattening of the toroidal rotation profile at tearing mode surfaces [77]. These internal modes can reach out and interact with even an axisymmetric boundary and cause braking of the overall rotation profile, as takes place with the RWM [4]. However, even with plasmas below any instability boundary the natural breaking of axisymmetry due to external imperfections, i.e. TF ripple and magnetic error fields, or purposely added perturbation fields, contribute to this added transport. The interplay of external perturbations with rotation can be complicated, because the rotation itself can tend to screen the plasma from the imperfections, or help stabilize any plasma mode that might be driven, whilst the perturbations apply a drag on the rotation.

The external magnetic perturbations are generally categorized as resonant, or nonresonant (NR). The resonant perturbations are such that the perturbation resonates in the interior of the plasma with $\vec{B}$ on a rational magnetic surface. These are more effective at interacting with the plasma than nonresonant perturbations because the mode rational surfaces can carry image currents. A present focus of experimental and theoretical work is understanding the magnitude of the resultant perturbation within the plasma, due to possible amplification, toroidal mode coupling, and shielding [101]. NR perturbations have a more subtle effect, primarily by breaking the toroidal canonical momentum invariant so that single particle guiding center orbits are no longer closed. One inherent NR perturbation is TF ripple [102,103].

TF ripple is a subject long addressed theoretically [104] but with a modicum of experiments due to practical difficulty. Recently, a series of controlled TF ripple experiments has been conducted in JET, with the ripple varied from the standard low JET value of 0.08% up to 1.0% [103]. The reduction of the NBI-driven co-I_p toroidal velocity across the entire minor radius is significant, even though the ripple is primarily in the outer region. This velocity reduction from the normal value is significant when raising the ripple to the nominal value expected for ITER, of 0.5%. Analysis shows that, experimentally, τ_ϕ is reduced relatively more than τ_E [103]. Since breaking axisymmetry induces nonambipolar particle transport [99,105], it can generate a radial E field that results in generation of rotation and not only a drag. This rotation is in the counter-I_p direction because generally ions ripple diffuse more rapidly than electrons and the plasma tends to charge up negatively. Consistent with this picture, at high ripple in the JET experiments the edge region has a counter-I_p velocity even though the NBI drive

is still in the co-direction, and the edge velocity is in the co-I_p direction at lower ripple [103].

In JT-60U the negative E field, and resulting negative velocity, induced by TF ripple was significant prior to the installation of Ferritic Steel Tiles (FTS) to reduce the ripple. Figure 7 shows the toroidal velocity profile in JT-60U without (w/o) and with the FSTs, with co-injected (positive) NBI torque [102]. In spite of the NBI, the plasma rotation is counter-Ip everywhere (negative), in this large volume plasma, with the separatrix surface ripple given as 1.7% (w/o) and 1% (with FSTs). Smaller volume plasmas in JT-60U have much lower ripple.

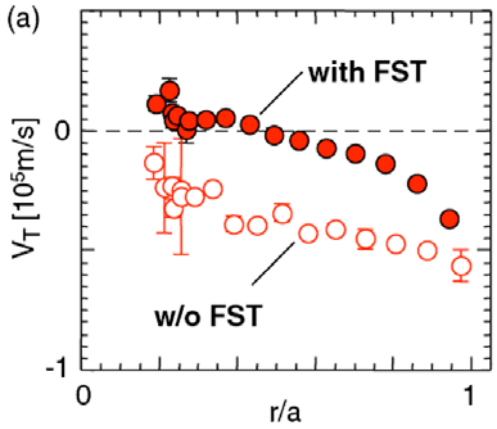

FIG. 7. The profiles of toroidal velocity I JT-60U with and without ferrite steel inserts. [Reprinted with permission from Urano H 2007 Nucl. Fusion **47**, P706, Copyright 2007, Institute of Physics.]

The nonambipolar radial current arising from NR perturbations is not a drag per se, it can exist without rotation, and as shown can dominate the rotation profile. This is a process related to the $J_f \times B$ torque we described above, under axisymmetric conditions, but it may be a region of phase space in the thermal population that is lost. The E field due to such thermal ion ripple loss has recently been measured in Tore Supra [106] and compared with theory in the steady state phase.

Another manifestation of a counter-I_p toroidal velocity generated by NR perturbations has been seen experimentally in DIII-D [107]. Magnetic perturbations with $n = 3$ and dominant m values in the range of 9–14 are applied in DIII-D, originally for the purpose of investigating ELM suppression [108]. If competing effects are small enough, these perturbations are theoretically predicted to lead to a steady state counter-I_p toroidal velocity due to neoclassical toroidal viscosity (NTV) [105]. This effect has been measured in DIII-D; velocities either more co-I_p than this "offset velocity", or more counter-I_p are observed to approach the offset value with application of the perturbation [107]. This value theoretically depends upon the collisionality regime, and the prediction

uses the standard NC result for poloidal velocity. Theory comparison is ongoing experimentally; the existence of an offset velocity has been established [107].

Both resonant and NR perturbations are contained in the error fields present at some magnitude in all tokamaks. Resonant error fields have long been known to be the trigger for so-called locked-modes, where the plasma ceases to rotate and may disrupt [109]. The drag on the plasma due to a resonant perturbation is a non-monotonic function of the toroidal velocity, and a simple model has been used to predict the catastrophic low rotation threshold that leads to locking [110].

VIII. PROJECTIONS TO ITER

While the present consensus is that "an ability to predict momentum transport and rotation for ITER is currently lacking" [111], we can nevertheless make some order of magnitude estimates based upon the empirical results described here. First, even with a model for transport and any turbulent sources an absolute rotation profile cannot be calculated apart from a boundary condition. This is an area that needs to be addressed more. Turbulence may provide a velocity in the large gradient pedestal region, or perhaps thermal ion orbit loss may possibly set a lower bound for the pedestal toroidal velocity [112,113].

To establish a scale of merit for rotation in ITER we consider the velocity normalized to the Alfvén velocity, V_A. A velocity of $M_A = V_\phi / V_A = 1\%$ is $V_\phi \sim 60$ km/s, for an inductive scenario [114], which is a rotation frequency of $f_\phi = \omega_\phi / 2\pi \sim 1.5$ kHz. It is possible that twice this value is necessary to affect stability, and higher for confinement issues. The following estimates do not include any reduction due to TF ripple.

Even with zero boundary $V_\phi(a)$, so-called no-slip, the NNBI source parameters project to produce a core rotation frequency of ~ 0.8 kHz with $V^p = 0$ and $\chi_\phi = \chi_i$ [115]. The momentum pinch greatly enhances this value, with peak rotation well beyond the figure of merit above, for pinch magnitudes even smaller than measured in JET [20]. These beams were planned to inject co-I_p torque [115].

The MCFD results are perhaps applicable to the ITER rf system. The C-Mod results give a core value of V_ϕ over twice that achieved with the Rice scaling in the L-mode conditions, as used in these experiments to date [59]. The result fits reasonably well with the theoretical estimate of Myra and D'Ippolito [116], which if applied to ITER projects to $V_\phi / P \sim 0.16\,(k_\parallel / \chi_\phi)$ (km/s)/MW, with the mode converted $k_\parallel$ in m^{-1} and χ_ϕ in m^2/s and we have used the wave frequency =50 MHz. At $k_\parallel / \chi_\phi = 40$ m^{-3} s, $V_\phi = 60$ km/s with $P = 10$ MW of mode converted power. This value of $k_\parallel / \chi_\phi$ is not overly optimistic, using $k_\parallel = 40$ m^{-1}, as in C-Mod at similar B to ITER, it is realized with a diffusivity of 1 m^2/s. The applicability of this theory [116] for MCFD requires further experimental confirmation.

Co-I_p directed LHCD in C-Mod generates a significant counter-I_p V_ϕ in the core [60]. The explanation proposed is a pinch of the resonant trapped electrons with generation of a core negative E field [60]. Such a theoretical model will likely predict the linear relationship between the driven V_ϕ and the LH driven current in steady state, as indicated experimentally [60], because the same rf force generates current drive and the particle pinch. The proportionality will depend upon the local momentum transport rate,

among other terms. Such an effect may be useful in ITER for creating velocity shear, but it is premature to make an estimate here.

We posit that the most certain rotation in ITER, apart from nonaxisymmetries, will come from the intrinsic process, since this requires no auxiliary systems. The question is how large it will be. The simple extrapolation from the present empirical international database dimensionless fit for M_A gives an optimistic value of $V_\phi \sim 120$ km/s for an inductive scenario, and larger for the non-inductive scenarios [71,117]. However, to firm up this prediction further inter-machine intrinsic rotation experiments are needed focused on a size scaling for intrinsic rotation.

For nonaxisymmetries, the NTV offset velocity may be significant in ITER because a set of perturbation coils for ELM suppression is being designed [8]. This velocity is in the counter-I_p direction and thus competes with some, and adds to others of the above effects. An estimate for ITER projects a core-offset frequency of $f_\phi \sim -1$ kHz [107].

REFERENCES

[1] R. Hemsworth, *et al.,* Nucl. Fusion **49**, 045006 (2009).

[2] P.W. Terry, Rev. Mod. Physics **72**, 109 (2000).

[3] K.H. Burrell, Phys. Plasmas **4**, 1499 (1997).

[4] A.M. Garofalo, *et al.,* Phys. Rev. Lett. **89**, 235001 (2002).

[5] R.J. Buttery, "Multimachine extrapolation of neoclassical tearing mode physics to ITER" submitted to Nucl. Fusion *(*2008).

[6] P.A. Politzer, *et al.,* Nucl. Fusion **48**, 075001 (2008).

[7] K.H. Burrell, *et al.,* to be published in Nucl. Fusion *(*2009).

[8] R.J. Hawryluk, *et al.,* Nucl. Fusion **49**, 065012 (2009).

[9] T.E. Evans, *et al.,* "Operating characteristics in DIII-D ELM-suppressed RMP H-modes with ITER similar shapes," Proc. 22nd IAEA Fusion Energy Conf. (Geneva) Paper EX/4-1, submitted to Nucl. Fusion *(*2009).

[10] A.M. Garofalo, *et al.,* Phys. Plasmas **16**, 056119 (2009).

[11] B. Coppi, Nucl. Fusion **42**, 1 (2002).

[12] J.E. Rice, *et al.,* Plasma Phys. Control. Fusion **50**, 124042 (2008).

[13] K. Ida, Plasma Phys. Control. Fusion **40**, 1429 (1998).

[14] J.S. deGrassie, *et al.,* Phys. Plasmas **14**, 056115 (2007).

[15] Nagashima, *et al.,* Nucl. Fusion **34**, 449 (1994).

[16] K. Ida, *et al.,* Phys. Rev. Lett. **74**, 1990 (1995).

[17] M. Yoshida, *et al.,* Phys. Rev. Lett. **100**, 105002 (2008).

[18] W.M. Solomon, *et al.,* Nucl. Fusion **49**, 085005 (2009).

[19] S.M. Kaye, *et al.,* Nucl. Fusion **49**, 045010 (2009).

[20] T. Tala, *et al.,* Phys. Rev. Lett. **102**, 075001 (2009).

[21] K.W. Gentle, *et al.,* Plasma Phys. Control. Fusion **29**, 1077 (1987).

[22] D.R. Baker, *et al.,* Nucl. Fusion **40**, 1003 (2000).

[23] C. Angioni, *et al.,* Phys. Plasmas **12**, 112310 (2005).

[24] R.D. Hazeltine, Phys. Fluids **17**, 961 (1974).

[25] A. Scarabosio, *et al.,* Plasma Phys. Control. Fusion **48**, 663 (2006).

[26] R.P. Seraydarian, *et al.,* Rev. Sci. Instrum. **48**, 663 (1988).

[27] F.L. Hinton and R.D. Hazeltine, Rev. Mod. Physics **48**, 239 (1976).

[28] R.C. Isler, *et al.,* Plasma Phys. Control. Fusion **36**, 171 (1994).

[29] K.W. Hill, *et al.,* Plasma and Fusion Res. **2**, S1067 (2007).

[30] A. Tsushima, *et al.,* Jpn. J. Appl. Phys. **47**, 8576 (2008).

[31] D. Testa, *et al.,* Phys. Plasmas **9**, 243 (2002).

[32] S.K. Wong, *et al.,* Phys. Plasmas **15**, 082503 (2008).

[33] K. Ida, *et al.,* Phys. Plasmas **8**, 1 (2001).

[34] K. Crombé, *et al.,* Phys. Rev. Lett. **95**, 155003 (2005).

[35] B.W. Rice, *et al.,* Rev. Sci. Instrum **70**, 815 (1999).

[36] T.L. Rhodes, *et al.,* Nucl. Fusion **39**, 1051 (1999).

[37] M.R. Wade, Nucl. Fusion **47**, S543 (2007).

[38] P.N. Yushmanov, *et al.,* Nucl. Fusion **30**, 1999 (1990).

[39] R.J. Goldston, *et al.,* J. Comput. Phys. **43**, 61 (1981).

[40] A. Pankin, *et al.,* Comp. Phys. Comm. **159**, 157 (2004).

[41] R.J. La Haye, *et al.,* Nucl. Fusion **48**, 054004 (2008).

[42] K.H. Burrell, *et al.,* Phys. Rev. Lett. **102**, 155003 (2009).

[43] P. Gohil, *et al.,* J. Phys: Conf. Series **123**, 012017 (2008).

[44] F. Wagner, Plasma Phys. Control. Fusion **49**, B1 (2007).

[45] J.W. Connor, *et al.,* Nucl. Fusion **44**, R1 (2004).

[46] P.C. de Vries, *et al.,* Nucl. Fusion **49**, 075007 (2009).

[47] S. Suckewer, *et al.,* Phys. Rev. Lett. **43**, 207 (1979).

[48] F.L. Hinton and M.R. Rosenbluth, Phys. Lett. A **259**, 267 (1999).

[49] K.-D. Zastrow, *et al.,* Nucl. Fusion **38**, 257 (1998).

[50] J.S. deGrassie, *et al.,* Phys. Plasmas **13**, 112507 (2006).

[51] K.G. McClements and A. Thyagaraja, Phys. Plasmas **13**, 042503 (2006).

[52] P. Helander, *et al.,* Phys. Plasmas **12**, 112503 (2005).

[53] M. Honda, *et al.,* Nucl. Fusion **49**, 035009 (2009).

[54] A.H. Boozer, Phys. Fluids **19**, 150 (1976).

[55] W.W. Heidbrink, *et al.,* Nucl. Fusion **48**, 084001 (2008).

[56] R.B. White, *et al.,* Phys. Fluids **26**, 2959 (1983).

[57] W.W. Heidbrink, *et al.,* submitted to Plasma Phys. Control. Fusion (2009).

[58] L.-G. Eriksson. *et al.,* Phys. Rev. Lett. **92**, 235001 (2004).

[59] Y. Lin, *et al.,* Phys. Rev. Lett. **101**, 235002 (2008).

[60] A. Ince-Cushman, *et al.,* Phys. Rev. Lett. **102**, 035002 (2009).

[61] A.J. Lieber, *et al.,* Phys. Fluids **31**, 687 (1988).

[62] R.R. Dominguez and G.M. Staebler, Phys. Fluids B **5**, 3876 (1993).

[63] J.E. Rice, *et al.,* Nucl. Fusion **41**, 277 (2001).

[64] I.H. Hutchinson, *et al.,* Phys. Rev. Lett. **84**, 3330 (2000).

[65] B.P. Duval, *et al.,* Phys. Plasmas **15**, 056113 (2008).

[66] S. Assas, *et al.,* Proc. 30th EPS Conference on Control. Fusion and Plasma Phys. St. Petersberg, ECA Vol. **27A**, IP-1.138; http://epsppd.epfl.ch/StPetersburg;PDF/P1_138.PDF (2003).

[67] J.E. Rice, *et al.,* Nucl. Fusion **39**, 1175 (1999).

[68] W.D. Lee, *et al.,* Phys. Rev. Lett. **91**, 205003 (2003).

[69] J.S. deGrassie, *et al.,* Phys. Plasmas **11**, 4323 (2004).

[70] L.-G. Eriksson and F. Porcelli, *et al.,* Nucl. Fusion **42**, 959 (2002).

[71] J.E. Rice, *et al.,* Nucl. Fusion **47**, 1618 (2007).

[72] M. Shimada, *et al.,* Nucl. Fusion **47**, S1 (2007).

[73] C.C. Petty, Phys. Plasmas **15**, 080501 (2008).

[74] F.L. Hinton and S.K. Wong, Phys. Fluids **28**, 3082 (1985).

[75] S. Newton and P. Helander, Phys. Plasmas **13**, 012505 (2006).

[76] S.D. Scott, *et al.,* Phys. Rev. Lett. **64**, 531 (1990).

[77] J.S. deGrassie, *et al.,* Nucl. Fusion **43**, 142 (2003).

[78] P.C. de Vries, *et al.,* Nucl. Fusion **48**, 065006 (2008).

[79] N. Mattor and P.H. Diamond, Phys. Fluids **31**, 1180 (1988).

[80] J. Weiland, *et al.,* Plasma Phys. Control. Fusion **49**, A45 (2007).

[81] W.X. Wang, *et al.,* Phys. Rev. Lett. **102**, 035005 (2009).

[82] K.C. Shaing, Phys. Plasmas **8**, 193 (2001).

[83] R.E. Waltz. *et al.,* Phys. Plasmas **14**, 122507 (2007).

[84] P.H. Diamond, *et al.,* Phys. Plasmas **15**, 01203 (2008).

[85] T.S. Hahm, *et al.,* Phys. Plasmas **15**, 072302 (2007).

[86] Ö.D. Gürcan, *et al.,* Phys. Rev. Lett. **100**, 135001 (2008).

[87] A.G. Peeters, *et al.,* Phys. Rev. Lett. **98**, 265003 (2007).

[88] Y. Camenen, *et al.,* Phys. Rev. Lett. **102**, 125001 (2009).

[89] C.J. McDevitt, *et al.,* Phys. Plasmas **16**, 052302 (2009).

[90] H.A. Claassen, *et al.,* Phys. Plasmas **7**, 3699 (2000).

[91] A.L. Rogister, *et al.,* Nucl. Fusion **42**, 1144 (2002).

[92] P.J. Catto and A.N. Simakov, Phys. Plasmas **12**, 114503 (2005).

[93] S.K. Wong and V.S. Chan, Phys. Plasmas **12**, 092513 (2005).

[94] J.S. deGrassie, *et al.,* Proc. 26th EPS Conf. on Controlled Fusion and Plasma Physics (Maastricht) Vol **23J**, (ECA) 1189 (2000).

[95] J.S. deGrassie, L.-G. Eriksson, and J.-M. Noterdaeme, Proc. 16th Top. Conf. on RF Power in Plasmas (Park City) Vol **787**, ed. S.J. Wukitch and P.T. Bonoli (Melville, American Institute of Physics) p 110 (2005).

[96] E.J. Doyle, *et al.,* Nucl. Fusion **47**, S18 Sec. 5.3 (2007).

[97] D. Nishijima, *et al.,* Plasma Phys. Control. Fusion **47**, 89 (2005).

[98] Sakamoto, *et al.,* Plasma Phys. Control. Fusion **48**, A63 (2006).

[99] A.H. Boozer, Phys. Plasmas **16**, 052505 (2009).

[100] J.A. Snipes, *et al.,* Nucl. Fusion **30**, 205 (1990).

[101] J.-K. Park, *et al.,* Phys. Plasmas **16**, 056115 (2009).

[102] H. Urano, *et al.,* Nucl. Fusion **47**, 706 (2007).

[103] P.C. de Vries, *et al.,* Nucl. Fusion **48**, 035007 (2008).

[104] P.N. Yushmanov, Nucl. Fusion **12**, 1599 (1983).

[105] A.J. Cole, *et al.,* Phys. Plasmas **15**, 056102 (2008).

[106] E. Trier, *et al.,* Nucl. Fusion **48**, 092001 (2008).

[107] A.M. Garofalo, *et al.,* Phys. Plasmas **16**, 056119 (2009).

[108] T.E. Evans, *et al.,* Nucl. Fusion **48**, 024002 (2008).

[109] T.C. Hender, *et al.,* Nucl. Fusion **32**, 2091 (1992).

[110] H. Reimerdes, *et al.,* "Effect of resonant and non-resonant magnetic braking on error field tolerance in high beta plasmas," submitted to Nucl. Fusion (2009).

[111] E.J. Doyle, *et al.,* Nucl. Fusion **47**, S18 Sec. 6 (2007).

[112] J.S. deGrassie, *et al.,* to be published in Nucl. Fusion (2009).

[113] C.S. Chang, and S. Ku, Phys. Plasmas **15**, 062510 (2008).

[114] B.J. Green, Plasma Phys. Control. Fusion **45**, 687 (2003).

[115] R.V. Budny, *et al.,* Nucl. Fusion **48**, 075005 (2008).

[116] J.R. Myra and D.A. D'Ippolito, Phys. Plasmas **9**, 3867 (2002).

[117] J.E. Rice, J. Physics: Conf. Series **123**, 012003 (2008).

.

ACKNOWLEDGMENTS

This work was supported by the US Department of Energy under DE-FC02-04ER54698.